Real and Reactive Power Control of a Three-Phase Single-Stage PV System and PV Voltage Stability

Huijuan Li, *Member, IEEE*; Yan Xu, *Senior Member, IEEE*; Sarina Adhikari, *Student Member, IEEE*; D. Tom Rizy, *Senior Member,* Fangxing Li*, Senior Member, IEEE*; Philip Irminger, *Student Member, IEEE*

***Abstract* — Grid-connected photovoltaic (PV) systems with power electronic interfaces can provide both real and reactive power to meet power system needs with appropriate control algorithms. This paper presents the control algorithm design for a three-phase single-stage grid-connected PV inverter to achieve either maximum power point tracking (MPPT) or a certain amount of real power injection, as well as the voltage/var control. The switching between MPPT control mode and a certain amount of real power control mode is automatic and seamless. Without the DC-to-DC booster stage, PV DC voltage stability is an important issue in the control design especially when the PV inverter is operating at maximum power point (MPP) with voltage/var control. The PV DC voltage collapse phenomenon and its reason are discussed. The method based on dynamic correction of the PV inverter output is proposed to ensure PV DC voltage stability. Simulation results of the single-stage PV system during system disturbances and fast solar irradiation changes confirm that the proposed control algorithm for single-stage PV inverters can provide appropriate real and reactive power services and ensure PV DC voltage stability during dynamic system operation and atmospheric conditions.**

***Index Terms*—**photovoltaic (PV) systems, maximum power point tracking (MPPT), DC voltage stability, distributed energy resources, single-stage PV inverter, smart inverter control, real power control, voltage control, reactive power, microgrid, smart grid**.**

I. Introduction

Photovoltaic (PV) system installations in the U.S. are booming at a high rate due to increased utility electric costs and incentives offered by state and federal governments. In 2010, the installed capacity of PV systems for electricity generation was 981 MW and 814 MW for thermal heating, doubling the capacity installed in 2009 [1]. For grid-connected PV systems, DC power from the PV array is converted to grid-compatible AC power at the appropriate voltage level and injected into the grid by power electronic converters. Generally, PV systems track the maximum power point (MPP) of the PV array to extract maximum available solar energy. However, PV systems may also have to follow dispatch commands to output a certain amount of real power or to participate in frequency regulation. In order to work in quite dynamic system conditions, PV systems need to seamlessly switch between fixed real power control mode and MPPT mode.

Currently, most PV systems operate at unity power factor due to the IEEE Std. 1547 Guide [12]. With the fast growth of PV systems and the fact that some utilities are experiencing high penetration levels of PV systems on distribution circuits, guidelines for voltage and reactive power (voltage/var) regulation from distributed energy resources (DER) are underway by the IEEE 1547.8 working group of SCC 21 [13] to identify the requirements for local voltage/var control by distributed generation and renewable energy. The reactive power support or voltage regulation potential of PV inverters could greatly benefit power system stability [2]-[5]. By utilizing the remaining capacity or slightly increasing the capacity of the inverter, PV systems can provide significant voltage/var support. Furthermore, the provision of reactive power does not require the availability of solar energy and can be at the PV inverter's full capacity when PV arrays are not generating any real power at night. For instance, if the a PV system is rated at 100 kVA with a 0.9 power factor, the real power output is 90 kW and the remaining reactive power capability is up to ±43.6 kVAr, or a range of 87.2 kVAr. This characteristic makes voltage/var control a more cost-effective service provided by PV systems than from other dynamic reactive power compensator such as STATCOM.

The most common PV interface configurations are two-stage converters and single-stage inverters. The two-stage converters consist of a DC-to-DC boost converter for the first stage, which boosts the PV array output DC voltage up for the second stage and performs MPPT or follows an real power reference. The second stage is an inverter, which generates the grid compatible AC voltage and provides voltage/var control. Single-stage inverters only consist of an inverter which controls the real and reactive power output as well as generates a grid compatible voltage. Typically, a single-stage inverter has higher power conversion efficiency, lower cost and higher reliability since the chance of component failure is lower with respect to the two-stage converter. However, without the DC voltage boost capability of the DC-to-DC converter, single-stage voltage sourced inverters (VSI) require higher DC voltage in order to provide voltage/var control [6]-[7]. Moreover, because of the varying DC voltage, the control algorithm is inevitably more complex in order to achieve simultaneous power flow control and power conversion in a single inverter.

H. Li is with Oak Ridge Associated Universities (ORAU) in the postdoctoral research associates program at Oak Ridge National Laboratory (ORNL).

Y. Xu is a researcher in the Power & Energy Systems Group at ORNL.

S. Adhikari is a PhD candidate at the University of Tennessee, Knoxville.

D. T. Rizy is a senior researcher in the Power & Energy Systems Group at ORNL.

F. Li is an associate professor at the University of Tennessee, Knoxville.

P. Irminger is with ORAU in the postBS research associates program at ORNL.

Contact: H. Li, 1-865-241-2598 (phone) or lih3@ornl.gov (email).

This manuscript has been authored by UT-Battelle, LLC, under Contract No. DE-AC05-00OR22725 with the U.S. Department of Energy.

978-1-4673-2729-9/12/$31.00 ©2012 IEEE

Many control algorithms have been developed for the MPPT control of PV systems. The most popular method in use is the perturb & observe (P&O) or hill climbing [8] method. A small perturbation is intentionally created by the MPPT control. If the output power increases after this perturbation, the next perturbation will be in the same direction as this one. Otherwise, the perturbation will be in the opposite direction. This method requires little calculation and is easy to implement. However, perturbations may be caused by other events other than the P&O control, such as solar irradiation changes and voltage regulation changes on the system. The P&O control is unable to distinguish the difference between all of these perturbations and therefore may make a wrong adjustment as a result. The changing rate in DC power to voltage (*dP/dV)* or current (*dP/dI*) is an indicator of the PV array operating point, which equals to zero at the maximum power point (MPP). With fast-acting microcontrollers like digital signal processors (DSP), *dP/dV* (or *dP/dI*) feedback control for MPPT can be implemented [7].

MPP is a critical steady point for DC voltage stability, considering the PV's current versus voltage characteristic. In the current source region, a small current increase will very likely cause a DC voltage collapse [9]. As a result, the PV system running near the MPP operating point is more sensitive to disturbances. Thus, maintaining the DC voltage stability is very important for a single-stage inverter implemented with voltage/var control function.

Basically, the control algorithm of grid-interfaced PV system needs to achieve these functions: (1) generate a grid-compatible sinusoidal waveform; (2) perform maximum power point tracking (MPPT) or follow a real power output reference; (3) if permitted such as per a finalized IEEE 1547.8 std., provide voltage regulation or follow a reactive power output reference; and (4) ensure PV DC voltage stability.

This paper presents a real and reactive power control algorithm for a three-phase single-stage PV inverter. The real power can be a MPPT or a fixed amount control, and the reactive power control can be a local voltage regulation control or a fixed amount of reactive power control. The MPPT control algorithm is based on a *dP/dV* feedback control. The proposed PV inverter control can automatically and seamlessly switch between fixed real power mode and MPPT control mode according to an operational command and/or atmospheric condition. A strategy for fast correction of the PV array operating point is introduced to ensure DC voltage stability. Section II briefly reviews PV system modeling while the control algorithm is proposed in Section III. The PV DC voltage stability issue is discussed in Section IV. Simulation results are presented in Section V and conclusions are drawn in Section VI.

II. PV Array Characteristics and Modeling

PV array characteristics and its mathematic model will be introduced in this section.

A PV array is composed of PV cells connected in series and in parallel to achieve the desired DC power and DC voltage input for an inverter system. Fig. 1 shows the current-voltage (*I-V*) curve of a PV array. The single-diode equivalent circuit of a PV array is shown in Fig. 2. The PV DC power vs. voltage characteristics at different solar irradiation levels and temperatures are shown in Figs. 3 and 4, respectively.

Three characteristic operation points for the PV system: open circuit, MPP and short circuit are shown in Fig. 1. I_{sc} is the short circuit current; V_{oc} is the open circuit voltage; V_{mpp} and I_{mpp} are voltage and current at the MPP, respectively. The corresponding mathematical equation is given in Eq. (1) [10][11].

$$I = I_{pv} - I_0\left[\exp\left(\frac{q(V+R_sI)}{N_skTa}\right)-1\right]-\frac{V+R_sI}{R_{sh}} \quad (1)$$

where I_{pv} and I_0 are the PV and the diode saturation currents, respectively. N_s is the number of cells connected in series for greater output voltage, k is the Boltzmann constant (1.3806503×10^{-23} J/K), T (Kelvin) is the temperature of the p-n junction of the diode, and q (1.60217646×10^{-19}C) is the electron charge. R_s and R_{sh} are the equivalent series and shunt resistances of the array, respectively, and a is the diode constant factor, which is usually chosen to be in the range of $1\leq a \leq 1.5$ [11].

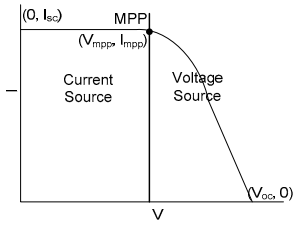

Fig. 1. Current-Voltage (*I-V*) characteristic curve of a PV array. [10]

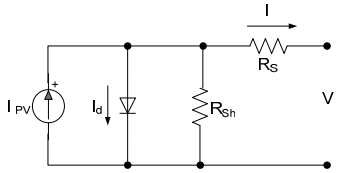

Fig. 2. Single-diode equivalent circuit of a PV array. [11]

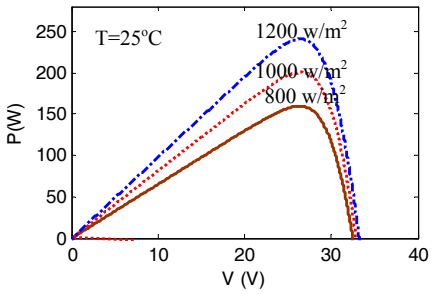

Fig. 3. PV DC power output vs. voltage at different solar irradiations.

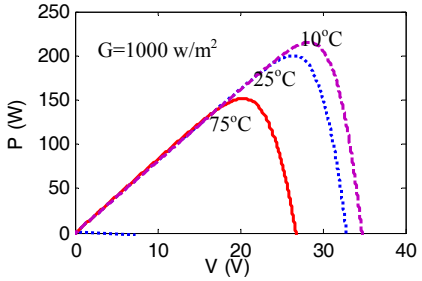

Fig. 4. PV DC power output vs. voltage at different temperatures.

Typically, the PV manufacturer's datasheet provides parameters I_{sc}, V_{oc}, I_{mpp}, V_{mpp}, and P_{max}, the maximum power, at a certain testing condition along with voltage and current temperature coefficients K_V and K_I. Therefore, the parameters used in a PV model are calculated using the datasheet information. Two of the most important parameters, R_s and R_{sh}, can be calculated by matching up the maximum output power of the model with that provided by the datasheet [11]. With the value of R_s and R_{sh}, the other parameters can be calculated as

$$I_{pv} = \left(I_{pv,n} + K_I \Delta T\right)\frac{G}{G_n} \tag{2}$$

$$I_0 = \frac{I_{sc}+K_I\Delta T}{\exp\left(\frac{V_{oc}+K_V\Delta T}{N_S kTa}\right)-1} \tag{3}$$

Where

$$I_{pv,n} = \frac{R_{sh}+R_s}{R_{sh}} I_{sc} \tag{4}$$

G and G_n are the actual and nominal solar irradiation, respectively; $\Delta T = T - T_n$, T_n is the nominal temperature.

The PV array output power varies with atmospheric conditions as shown in Figs. 3 and 4. PV arrays generate more power with higher solar irradiations. Thus, the PV array current is more sensitive to solar irradiation change than the voltage. As indicated in Fig. 4, the PV array output power increases while the temperature drops. The PV array output voltage is more sensitive to the temperature changes than the current.

As shown in Figs. 1, the PV array has two distinct operating regions, the current source region on the left, and the voltage source region on the right side of the MPP. In the current source region, the PV output current is higher and almost constant while the voltage is lower relative to the voltage source region. In the voltage source region, the PV output current is lower, and the voltage is higher and with lower variation relative to the current source region.

III. Control of Real and Reactive Power Output of Single-Stage PV System

The configuration of a three-phase single-stage PV system connected to the utility grid is shown in Fig. 5. The power electronic interface has a DC-to-AC converter, and does not have a DC-to-DC converter for boosting the DC voltage. The PV array which is shown in the figure supplies DC power to the inverter at a voltage level of v_{pv} and current level i_{pv}. A DC link capacitor C is located between the PV array and the inverter. The PV inverter is connected through a transformer with equivalent inductance L_c at the point of common coupling (PCC) to the grid. The PCC voltage is v_t while the PV inverter output voltage and current are v_c and i_c, respectively. The utility grid is simplified as a voltage source, v_s, with a system impedance of $R_s + j\omega L_s$. The current to the local load connected in parallel with the PV inverter is i_l. Both the phase angle and magnitude of the inverter output voltage, v_c are controlled to regulate the PV inverter real power and the reactive power supplied to the grid. The PV inverter real power is equal to the

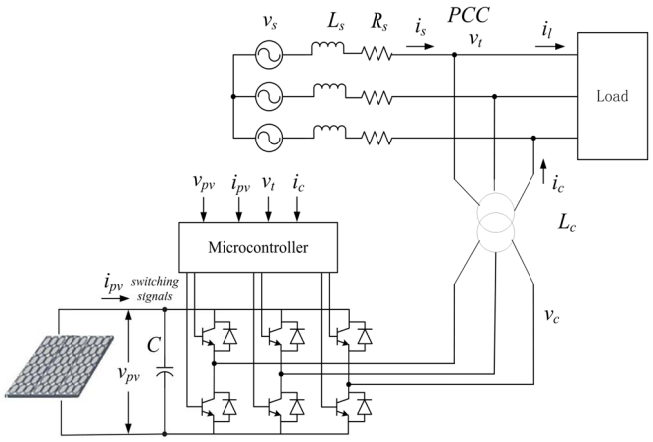

Fig. 5. A grid-connected three-phase single-stage inverter PV system.

PV array output power less the inverter losses because of the energy balance between PV inverter DC input and AC output.

The instantaneous active current i_{ca}, real power p, reactive current i_{cn}, and reactive power q, can be calculated from measurements of the inverter current, i_c, and voltage, v_t as:

$$i_{ca}(t) = \frac{\frac{1}{T}\int_{t-T}^{t} v_t^T(\tau)\cdot i_c(\tau)d\tau}{V_t^2(t)}\, v_t(t). \tag{5}$$

$$i_{cn}(t) = i_c(t) - i_{ca}(t) \tag{6}$$

$$p(t) = v_t^T(t) i_{ca}(t) \tag{7}$$

$$q(t) = v_t^T(t) i_{cn}(t) \tag{8}$$

The average real power and average reactive power output of the PV inverter to the grid can be expressed as Eqs. (9) and (10), respectively. When the phase angle α between the PCC voltage and inverter output voltage is small, they can be approximated by the second expression of Eqs. (9) and (10).

$$P = \frac{V_t V_c}{X_l}\sin\alpha \approx \frac{V_t V_c}{X_l}\alpha \tag{9}$$

$$Q = \frac{V_t}{X_l}(V_c\cos\alpha - V_t) \approx \frac{V_t}{X_l}(V_c - V_t) \tag{10}$$

where V_t and V_c are the RMS values of the PCC terminal voltage v_t, and inverter output voltage v_c, α is the phase angle difference of v_c and v_t, and X_l is the equivalent reactance of the transformer.

Hence, we can see that the real power flow is controlled by regulating the phase angle α of v_c and the reactive power is controlled by regulating the amplitude of v_c.

A. *Fixed Real Power and Voltage/Var Control*

The real power and reactive power of the PV inverter can be controlled simultaneously and independently. Depending on the control objectives, the MPP of the PV arrays or a fixed amount of real power could be the control goal for the real power control. For the reactive power, the control goal could be maintaining the local PCC voltage at some reference setting or providing a fixed amount of reactive power. In this paper, a proportional-integral (PI) feedback control is implemented in the PV system controller. Fig. 6 shows the logic used to

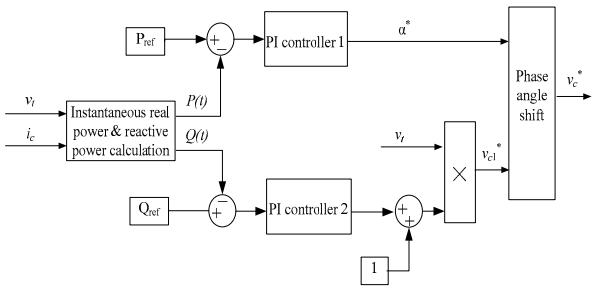

Fig. 6. Fixed real power and voltage/var control of the PV system.

achieve the fixed real power and reactive power control of the PV inverter, which is expressed in Eqs. (11) and (12).

The PI_1 controller is used to control the real power while the PI_2 controller is used to control the reactive power. The instantaneous real power and reactive power are calculated using Eqs. (5)-(8) and compared with a real power reference, P_{ref}, and reactive power reference, Q_{ref}, respectively. The errors in the power output are fed into their respective PI controllers to minimize the error between the actual and reference values. The signal generated by the real power PI controller regulates the phase angle of the inverter output voltage (v_c) while the signal from the reactive power PI controller adjusts the amplitude of v_c.

$$\alpha^* = K_{P1}\left(P_{ref} - P(t)\right) + K_{I1}\int_0^t \left(P_{ref} - P(\tau)\right) d\tau. \quad (11)$$

$$v_{c1}^* = \left[1 + K_{P2}\left(Q_{ref} - Q(t)\right) + K_{I2}\int_0^t \left(Q_{ref} - Q(\tau)\right) d\tau\right] v_t(t) \quad (12)$$

The local PCC voltage control is implemented by replacing the reactive power reference signal, Q_{ref} , of the control logic in Fig. 6 with the PCC voltage reference signal, V_{ref}. The control logic for the fixed real power and voltage control is shown Fig. 7. Eq. (13) gives the corresponding expression.

$$v_{c1}^* = \left[1 + K_{P2}\left(V_{t\_ref} - V(t)\right) + K_{I2}\int_0^t \left(V_{t\_ref} - V(\tau)\right) d\tau\right] v_t(t) \quad (13)$$

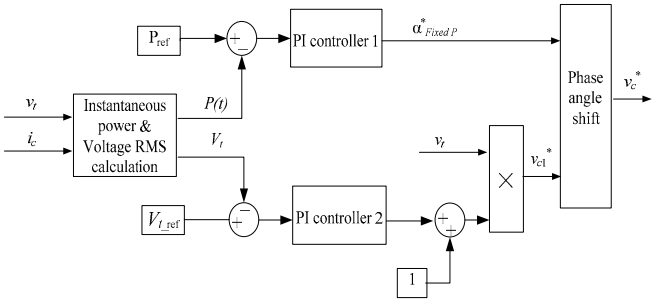

Fig. 7. Fixed real power and voltage control of PV array.

B. MPPT Control

A characteristic of the PV array operations in regards to MPPT is utilized in the controls presented in this paper. It is the fact that at the MPP, dp_{pv}/dv_{pv}=0. With a microcontroller's high-speed calculation capability, a feedback control with the objective of keeping dp_{pv}/dv_{pv} at or near zero can be achieved and is utilized in this paper. Fig. 8 shows the MPPT control logic implemented with a PI controller, which is also expressed in Eq. (14) in which dp_{pv}/dv_{pv} is approximated with $\Delta p_{pv}/\Delta v_{pv}$. The PI controller generates the phase shift reference of the inverter output voltage v_c to keep $\Delta p_{pv}/\Delta v_{pv}$ close 0. MPPT can be achieved simultaneously with either the reactive power control or voltage control. As indicated earlier, the reactive power control or voltage control is achieved by regulating the magnitude of v_c .

$$\alpha^* = -K_P\frac{\Delta p_{pv}(t)}{\Delta v_{pv}(t)} - K_I\int_0^t \frac{\Delta p_{pv}(\tau)}{\Delta v_{pv}(\tau)} d\tau \quad (14)$$

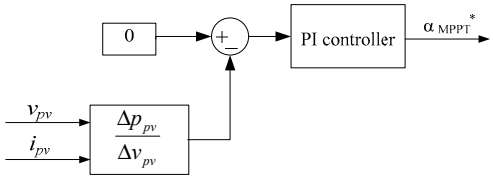

Fig. 8. MPPT control

In the voltage source region, $dp_{pv}/dv_{pv} < 0$ and according to Eq. (14), α^* increases, causing PV inverter to increase real power output and the capacitor of the DC link will discharge. As a result, the DC voltage will decrease and the PV array operating point moves to the MPP. If the PV array moves beyond the MPP and into the current source region, $dp_{pv}/dv_{pv} > 0$ and α^*decreases, causing PV inverter to decrease real power output. When the PV inverter real power output is less than the PV array output power, the capacitor will be charged. As a result, the DC voltage will increase and the PV array operating point will move toward the MPP. However, in the current source region, the DC voltage keeps decreasing until the PV inverter real power output decrease to less than the PV array output power. In some cases, the PV DC voltage may decrease to an unacceptable low level. Additional correction measures are introduced to address this issue, which is discussed in Section IV.

C. Switching between Fixed Real Power Mode and MPPT Control Mode

The PV system needs to be able to seamlessly switch between fixed real power control mode and MPPT control mode. For instance, a PV system initially follows a dispatch command per the system operator and is operated in the fixed real power control mode. Later a cloud blocks the sun and causes the PV array's maximum power to drop below the fixed real power setting. In this scenario, if the control cannot be quickly switched from fixed real power to MPPT, the control will eventually collapse. On the other hand, in some cases such as during a light load level, the PV array needs to reduce the real power output to prevent the PCC voltage increase. In this situation, the PV system needs to switch to operating at the fixed real power control mode. Generally, seamless switching between fixed real power and MPPT control is necessary for PV systems to operate smoothly during dynamic atmospheric and power grid conditions. Fig. 9 shows the logic used to achieve the seamless switching of these control modes. Eq. (15) provides the logic used for overall phase angle shift adjustment.

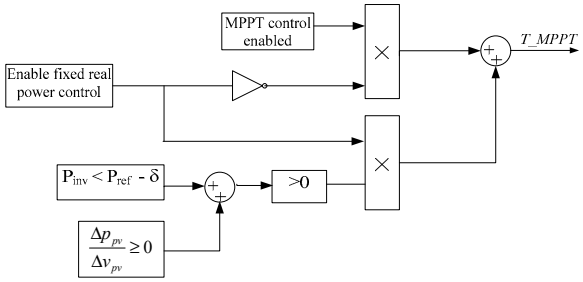

Fig. 9. Switching between fixed real power control and MPPT control.

$$\alpha^* = T\_MPPT * \alpha^*_{MPPT} + (1 - T\_MPPT) * \alpha^*_{Fixed\ P} \qquad (15)$$

where,

$$T\_MPPT = \begin{cases} 1; & if\ MPPT\ control \\ 0; & if\ Fixed\ real\ power\ control \end{cases}$$; and

α^* is the overall phase angle shift; α^*_{MPPT} is phase angle shift from the MPPT control; $\alpha^*_{Fixed\ P}$ is the phase angle shift from fixed real power control.

An external fixed real power control command is given higher priority than the MPPT control. When the fixed real power control is enabled, the PV inverter output power p and the derivative $\Delta p_{pv}/\Delta v_{pv}$ are closely watched to determine which mode should be in operation. When $\Delta p_{pv}/\Delta v_{pv}$ is equal to or slightly larger than 0, it means that the PV inverter output power is on the edge of maximum power limit and MPPT control needs to be switched on. When the PV output power is well below the fixed real power reference, regardless of the value of $\Delta p_{pv}/\Delta v_{pv}$, the MPPT control is engaged. If the PV inverter real power is approaching P_{ref} and falls into a tolerance range, δ, the fixed power control will be activated.

IV. PV Voltage Stability in MPPT Control

Fig. 10 shows the different operation regions of a PV system. Assume that initially the PV array is operating at the MPP with the output power p_m and voltage v_m, respectively, as shown in Fig. 10. The disturbances to the MPPT control fall into the three types: atmospheric changes including temperature and solar irradiation changes, impact from the transient during a process of voltage/var control and any disturbances from power grid that cause the PCC voltage

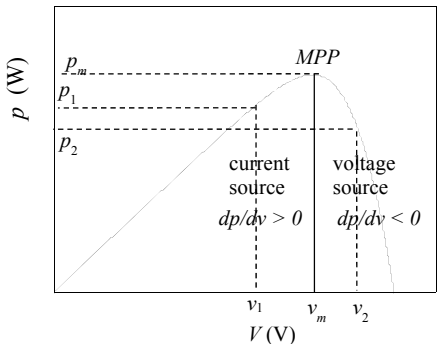

Fig. 10. PV array operation regions.

change. Usually, the changing rate of sun irradiation and ambient temperature is in the range of a few seconds, while the PI controller speed is in milliseconds or even microseconds range. Therefore, the sun irradiation and ambient temperature can be considered as constants during the electrical circuit responses and control transients. Because the real power and the reactive power control of the inverter are not completely decoupled, especially during a transient, both the real power control and the voltage/var control have impact on the DC link and hence the DC voltage, and may result in stability problem. The grid electrical change is almost instantaneous and causes a step-change-like disturbance on the MPPT control. As a result, the capacitor on the DC link will be greatly impacted and DC voltage may drop significantly. For instance, a sudden PCC voltage increase causes the PV inverter to output more real power than p_m, and the capacitor on the DC link of the inverter will discharge to make up for the power deficiency, which results in a decrease of the DC voltage. The PV array operating point hence moves to the current source region and the PV array output power decreases to p_1 resulting a larger deficiency between the PV inverter output power and the PV array available power. As discussed before, if the PV inverter real power output is not decreased below the PV array output power very quickly, the capacitor will further discharge and the operating point on the P-V curve drops further down on the left side of the MPP and eventually the PV DC voltage drops to an unacceptable level before it starts to increase. Generally, any disturbances, which cause the capacitor on the DC link to discharge significantly, will result in DC voltage stability problem.

Fig. 11(a) shows the DC voltage collapse phenomenon of a PV array operating at the MPP with voltage regulation when the voltage reference of the controller is increased by 1.7 V. The disturbance to the PV DC voltage caused by the new voltage regulation setting pushes the PV array operating point far into the current source region, which is shown by the large positive value of dp_{pv}/dv_{pv} in Fig. 11(b).

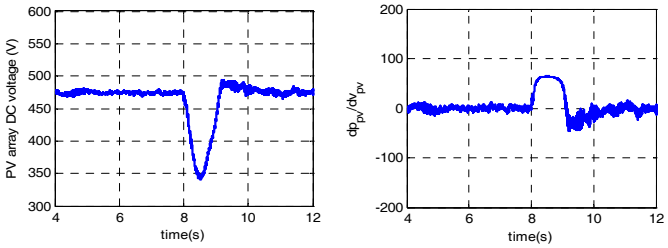

(a). PV array voltage collapse (b). *dp/dv* value

Fig. 11. PV array DC voltage collapse phenomenon.

If some correction measures are taken right after the disturbance to reduce PV inverter real power output less than p_m, the capacitor will be charged and as a result, the DC voltage will increases to v_2 in Fig. 10 and PV array operating point moves to voltage source region. Then, MPPT control logic will increase PV inverter output real power and eventually the PV array operating point will return to MPP.

The value of dp_{pv}/dv_{pv} indicates the status of the PV array DC voltage stability. A large positive value of dp_{pv}/dv_{pv} results in a DC voltage collapse. Therefore, the objective is to keep the dp_{pv}/dv_{pv} from increasing to a large positive value or to be able to quickly push it back to a small positive or negative value in order to prevent a DC voltage collapse. The simple PI feedback MPPT control presented in the previous section can

keep the dp_{pv}/dv_{pv} at a low positive or negative value so that the PV system is operated within a tight tolerance around the MPP for small disturbances. However, for large sudden disturbances, the speed of the PI controller with fixed gains may not be fast enough to avoid DC voltage collapse. Hence, additional control logic providing fast correction of dp_{pv}/dv_{pv} value is needed to maintain DC voltage stability. This additional logic to keep the DC voltage stable is expressed in Eq. (16).

$$\alpha_{corrected}{}^{*} = \alpha_0^{*} - (\sum_0^k \beta_k) \tag{16}$$

Where $\alpha_{corrected}{}^{*}$ is the overall phase angle shift; $\alpha_0{}^{*}$ is the phase angle shift generated by the real power control; β_k is the phase angle correction shift increment at the k^{th} time step; the total phase angle shift correction is the accumulation of all the increments over the control time. β_k is a linear function of dp_{pv}/dv_{pv}, as shown in Fig. 12. The threshold, μ, at which this function engages is also shown. When dp_{pv}/dv_{pv} is less than μ, there is no correction increment at this step; otherwise, a correction increment proportional to dp_{pv}/dv_{pv} is applied.

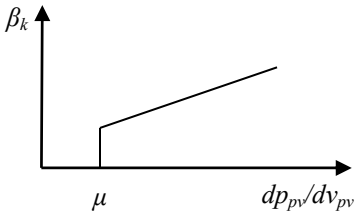

Fig. 12 Correction increment vs. dp_{pv}/dv_{pv}.

The dp_{pv}/dv_{pv} correction logic is a supplement to the fixed-gain PI controller based MPPT control, and it accelerates the control speed of reducing PV inverter real power output to a safe range to prevent a DC voltage collapse.

V. Simulation Results

The simulations of the real and reactive power control of the PV system under atmospheric condition changes are demonstrated in this section. The configuration of the simulation system is shown in Fig. 5. The PCC line-to-line voltage is 480 V and the load is 87 kVA (78 kW, 39 kVAr). The PV system is composed of solar arrays with 8 parallel connections and 18 serial connections. Table I shows the parameters of the PV module [11]. The maximum power of the PV arrays is around 28.8 kW. Simulations are done with power system transients simulation software EMTP-RV. An overview of the simulation model is shown in Fig.13. The controllers' parameters used in the simulations are listed in Table II.

Table I Parameters of the solar module at 25°C, A.M 1.5, 1000 W/m

I_{mp} (current at MPP)	7.61 A
V_{mp} (voltage at MPP)	26.3 V
$P_{max,e}$ (maximum electrical power)	200.143 W
V_{oc} (open circuit voltage)	32.9 V
I_{sc} (short circuit current)	8.21 A

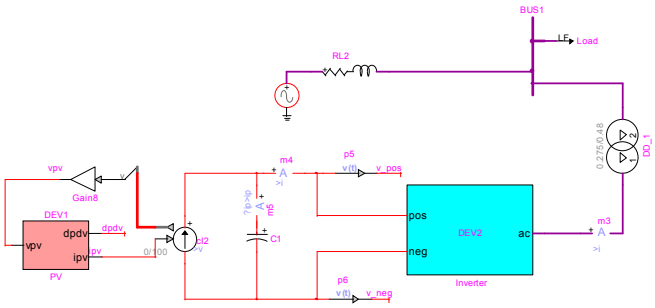

Fig. 13 Simulation model in EMTP-RV.

Table II. Gains for PI controllers

	K_P	K_I
MPPT control	1×10^{-9}	1×10^{-8}
Fixed amount of P control	5×10^{-8}	5×10^{-7}
Fixed amount of Q control	1×10^{-6}	1×10^{-5}
Voltage control	1×10^{-2}	1×10^{-1}

A. Fixed Real Power and Reactive Power/Voltage Control

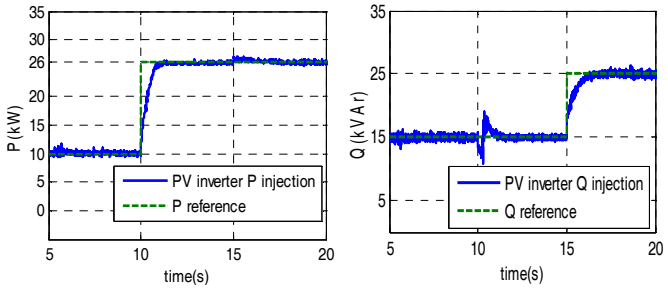

(a). PV inverter real power (b). PV inverter reactive power

Fig. 14 Fixed real and reactive power control.

Figs. 14(a) and (b) show the simulation results for the fixed real power and reactive power output control of the PV array. As shown in Fig. 14(a), at 10 s, a 16 kW step change is applied to the real power reference. The PV array real power output tracks this change and increases to 26 kW. The PV reactive power output also tracks its reference change, as shown in Fig. 14(b), which has been increase by 10 kVAr at 15 s.

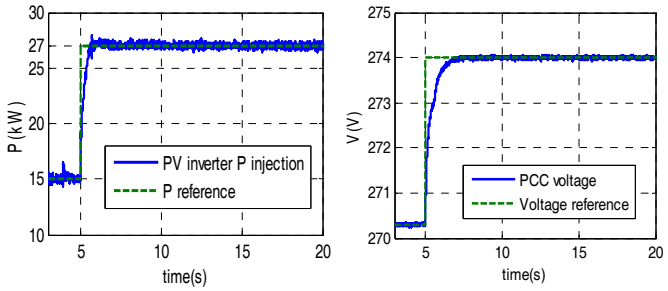

(a). PV inverter real power (b). PCC voltage RMS

Fig. 15 Fixed real power and PCC voltage control.

Figs. 15(a) and (b) show the fixed real power control of the PV system and the PCC voltage control. The references for real power and PCC voltage change simultaneously at time 5s. The real power reference is increased by 12 kW while the

voltage reference is increased by 3.7 V. The PV system real power and PCC voltage track the reference changes.

B. MPPT and Reactive Power/Voltage Control

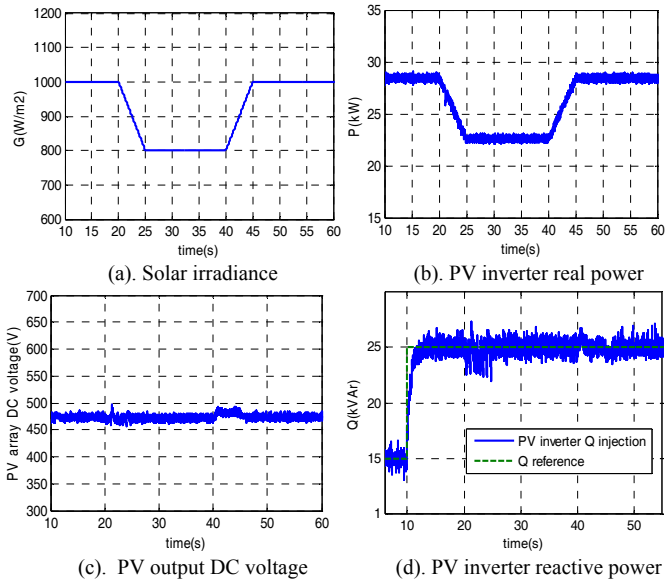

(a). Solar irradiance (b). PV inverter real power

(c). PV output DC voltage (d). PV inverter reactive power

Fig. 16. PV array MPPT and reactive power control under solar irradiance change.

Figs. 16(a), (b), (c) and (d) show the simulation results of the MPPT and fixed reactive power control of the PV system. Solar irradiance is constant at 1000 W/m^2 prior to 20 s. As shown in Fig. 16(d), at 10 s, a 10 kVAr step change is applied to the reactive power reference, and the reactive power control tracks this reference change and reaches a new steady state while the real power output is kept at its maximum setting of 28.8 kW as shown in Fig. 16(b). From 20 s to 25 s, the solar irradiance reduces from 1000 W/m^2 to 800 W/m^2, as shown in Fig. 16(a), and the maximum real power output decreases as well, as shown in Fig. 16(b), following the same pattern. From 25 s to 40 s, the solar irradiance does not change, the real power and reactive power output of the PV system thus remain constant. From 40 s to 45 s, solar irradiance increases back to 1000 W/m^2, and the PV array real power output also restores to its original 28.8 kW output level. The PV array DC voltage, as shown in Fig. 16(c), experiences small variations but is still stable during the two transitions. The reactive power experiences variations during both transitions because it is not fully decoupled from the impacts of real power control.

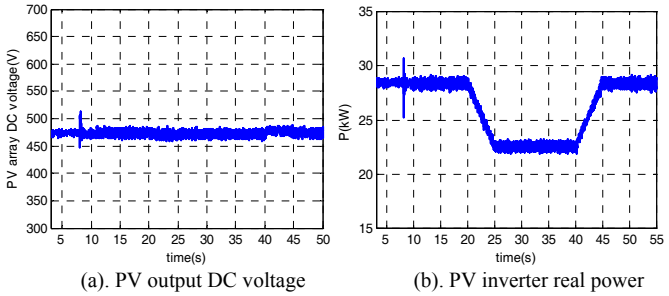

(a). PV output DC voltage (b). PV inverter real power

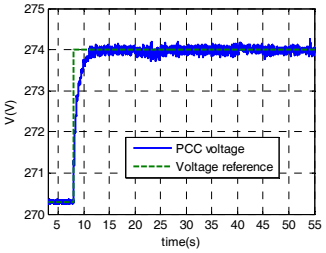

(c). PCC voltage RMS

Fig. 17. PV array MPPT and PCC voltage control under solar irradiance change.

Figs. 17(a), (b) and (c) show the simulation results of the PV array MPPT control and the PCC voltage control. In the previous case, the irradiance varies the same as well as the real power. Similar to the results of MPPT and reactive power control, in this case, the MPPT control can track the maximum power under atmospheric condition changes, and the PCC voltage can follow the reference change. A sudden PCC voltage reference change is applied at 8 s, as shown in Fig. 17(c), which imposes a large disturbance on the MPPT control. It can be seen from the real power output spike in Fig. 17(b). The DC voltage experiences a small dip following the sudden PCC voltage reference change; however, it is quickly brought back to a high level by the controller. These results show that the PV DC voltage stability is ensured by the controls during large disturbances.

C. Switching between Fixed Real Power Control and MPPT

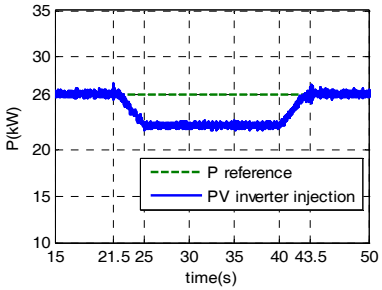

Fig. 18. Switching between fixed real power control and MPPT control.

Fig. 18 shows the simulation results of the PV system control when it switches between fixed real power control and MPPT control. The PV system is initially operating in fixed real power control mode with the real power reference set to 26 kW. From 20 s to 25 s, the solar irradiance reduces from 1000 W/m^2 to 800 W/m^2, the same as that shown in Fig. 16(a). The real power output is maintained at 26 kW when the available maximum power is larger than this amount prior to 21.5 s. After the solar irradiance decreases and the maximum power declines below 26 kW, the control switches to MPPT control to maintain output until the solar irradiance level returns to 1000 W/m^2. From 40 s to 45 s, the solar irradiance increases from 800 W/m^2 to 1000 W/m^2, so the control switches back to fixed real power control and the real power output restores to 26 kW at 43.5 s.

VI. CONCLUSIONS

This paper presents control algorithms for real power, reactive power and local voltage control of a grid-connected

three-phase single-stage photovoltaic (PV) system. The real power can be controlled either in the fixed real power mode or MPPT control mode, and the controller automatically switches between the two modes according to the system operator control commands or grid conditions. The potential DC voltage collapse problem associated with PV systems operating at MPP and being subject to large disturbances is addressed, and an effective prevention method is proposed and demonstrated. Simulation results of the fixed real power control, MPPT control, and switching between the two different operating modes confirm that the proposed control algorithm for the single-stage PV inverter has great scalability, adaptability, and can accommodate a wide range of atmospheric conditions and dynamic PV system operations as well. The developed control algorithms demonstrate that inverter-based PV systems can provide fast, local reactive power or voltage regulation support of distribution systems with a high PV penetration. Also the ability to switch between different operation modes automatically and seamlessly provides a means for the distribution system operator to deliver control schedules or commands to coordinate multiple PV systems.

VII. REFERENCES

[1] "U.S solar market trends 2010," Available online: http://www.irecusa.org/wp-content/uploads/2011/06/IREC-Solar-Market-Trends-Report-June-2011-web.pdf, Retrieved: Month, Year.

[2] H. Li, F. Li, Y. Xu, D. T. Rizy and J. D. Kueck, "Adaptive voltage control with distributed energy resources: algorithm, theoretical analysis, simulation, and field test verification", *IEEE Transactions on Power Systems*, vol.25, no.3, pp.1638-1647, Aug. 2010.

[3] Yan Xu, L. M. Tolbert, F. Z. Peng, J. N. Chiasson, and J. Chen, "Compensation-based non-active power definition," *IEEE Power Electronics Letters*, vol. 1, no. 2, June 2003, pp. 45-50, June 2003

[4] Sarina Adhikari, Yan Xu, Fangxing Li, Huijuan Li, John D. Kueck, Isabelle B. Snyder, Thomas J. Barker and Ronald Hite, "Utility-Side Voltage and PQ Control with Inverter-based Photovoltaic Systems," *Proc., the 18th IFAC World Congress*, Milano, Italy, 2011.

[5] D.T. Rizy, Huijuan Li, Fangxing Li, Yan Xu; S. Adhikari and P. Irminger, "Impacts of varying penetration of distributed resources with & without volt/var control: case study of varying load types," *Proc., IEEE Power and Energy Society General Meeting*, Detroit, MI, 2011

[6] H. Ribeiro, F. Silva, S. Pinto and B. Borges, "Single-stage inverter for PV applications with one cycle sampling technique in MPPT algorithm," in *Proc., 35th Annual IEEE Cof. on Industrial Electronics (IECON)*, Porto, Portugal, 2009.

[7] Riad Kadri, Jean-Paul Gaubert, "An improved maximum power point tracking for photovoltaic grid-connected inverter based on voltage oriented control," *IEEE Transactions on Industrial Electronics,* vol.58, no.1, pp.66-75, Jan. 2011.

[8] Trisham Esram and Patrick L. Chapman, "Comparison of photovoltaic array maximum power point tracking techniques," *IEEE Transactions on Energy Conversion*, vol.22, no,2, pp.439-449, June 2007.

[9] Libo Wu, Zhengming Zhao and Jianzheng Liu, "A single-stage three-phase grid-connected photovoltaic system with modified MPPT method and reactive power compensation," *IEEE Transactions on Energy Conversion*, vol. 22, no. 4, pp.881-886, December 2007.

[10] Felix A Farret and M. Godoy Simoes, "Integration of alternative sources of energy," A Wiley- Interscience Publication.

[11] Marcelo Gradella Villalva, Jonas Rafael Gazoli and Ernesto Ruppert Filho, "Comprehensive approach to modeling and simulation of photovoltaic arrays," *IEEE Transactions on Power Electronics,* vol.24, no.5, pp.1198-1208, May. 2009.

[12] http://grouper.ieee.org/groups/scc21/1547/1547_index.html, IEEE 1547 Standard for Interconnecting Distributed Resources with Electric Power Systems.

[13] http://grouper.ieee.org/groups/scc21/1547.8/1547.8_index.html, IEEE P1547.8 Recommended Practice for Establishing Methods and Procedures that Provide Supplemental Support for Implementation Strategies for Expanded Use of IEEE Standard 1547.